*Int. J. Heat Mass Transfer.* Vol. 32, No. 2, pp. 361–378, 1989
Printed in Great Britain

0017–9310/89 $3.00 + 0.00


# Predicting the onset of nucleate boiling in wavy free-falling turbulent liquid films

W. J. MARSH and I. MUDAWAR
Boiling and Two-phase Flow Laboratory, School of Mechanical Engineering,
Purdue University, West Lafayette, IN 47907, U.S.A.

(*Received* 6 *April* 1988 *and in final form* 6 *July* 1988)

**Abstract**—Experiments are performed to develop a fundamental understanding of boiling incipience in wavy free-falling turbulent liquid films. Incipience conditions are measured and correlated for water and a fluorocarbon (FC-72) liquid. Incipience in water films is influenced by turbulent eddies and, to a larger extent, by interfacial waves. A new approach to predicting incipience in water and other non-wetting fluids is presented. This approach utilizes physical parameters of commonly accepted incipience models and provides a means of correcting these models for the effects of turbulent eddies and roll waves. This study also demonstrates some unique incipience characteristics of fluorocarbon films. The weak surface tension forces of FC-72 allow droplets and liquid streams to break off the crests of incoming roll waves prior to, and during nucleate boiling. The low contact angle of FC-72 allows the liquid to penetrate deep inside wall cavities. Thus incipience from these flooded cavities requires much higher wall superheat than predicted from incipience models.

## 1. INTRODUCTION

FALLING liquid film flow is commonly encountered in many industrial applications involving condensation or evaporation such as chemical distillation, two-phase heat exchangers, and cooling systems for nuclear fuel rods and electronic packages. In many of these applications, it is very important to be able to predict the operating conditions which trigger nucleate boiling at the wall. The onset of nucleate boiling (ONB) defines the upper performance limit for some distillation devices, while in many other systems nucleate boiling is essential for increasing heat transfer effectiveness, and boiling incipience represents a lower bound for reliable operation.

Extensive numerical and experimental sensible heat transfer studies in falling films have been performed [1–6]. Falling films undergoing interfacial evaporation have also been studied by Chun and Seban [7], Fujita and Ueda [8] and Shmerler and Mudawwar [9]. Most of these studies utilized water as the working fluid and focused on film flow in the transitional or fully turbulent film regions.

Nucleate boiling in thin stationary liquid films was investigated by Mesler [10]. He identified microlayer evaporation as the mechanism by which a higher heat flux can be transferred from a hot surface to a thin film compared to other boiling systems at similar wall temperatures. He indicated that thin liquid films allow bubbles to escape quickly by bursting at the free interface. Thus, he hypothesized that microlayer evaporation is active over a longer fraction of the bubble contact time with the surface. However, it is not clear from these observations how microlayer evaporation influences the wall heat flux at the point of incipience.

Recent studies by Cerza and Sernas [11, 12] have concentrated on boiling nucleation criteria in developing laminar falling films. Their experiments involved film Reynolds numbers from 670 to 4300 using saturated water at atmospheric pressure. They determined that the pool boiling nucleation criterion (also known as the Clapeyron criterion) was applicable to falling water films. Fujita and Ueda's [8] study on nucleate boiling in saturated water films provided heat transfer coefficient correlations for films with little or no boiling and for films with fully developed nucleate boiling. Their boiling data covered a Reynolds number range of 700 to 9000; however, their study did not address conditions at the onset of nucleate boiling.

Although the number of studies addressing boiling incipience in falling films is limited, incipience in forced convection systems has been studied extensively during the last three decades. Early works by Sato and Matsumura [13], Bergles and Rohsenow [14], Davis and Anderson [15] and Yin and Abdelmessih [16] predicted incipience based on the point of tangency between the liquid temperature profile in the vicinity of the heated surface and the superheat temperature profile required for mechanical equilibrium of a vapor bubble growing at a surface cavity. The validity of this criterion was proven in many practical applications where the fluid is not highly wetting and where a wide range of surface cavity sizes exists on the boiling surface. A different hypothesis was used by Hino and Ueda [17] in their R-113 forced convection study, and by Sudo *et al.* [18] in their water forced convection study, who predicted incipience based on the maximum cavity radius available for nucleation on the heated surface. However, none of those two

## NOMENCLATURE

| | |
|---|---|
| $g$ | acceleration due to gravity |
| $h_E$ | heat transfer coefficient for evaporative heating, $q/(T_w - T_{sat})$ |
| $h_{fg}$ | latent heat of vaporization |
| $h_H$ | heat transfer coefficient for sensible heating, $q/(T_w - T_m)$ |
| $h_E^*$ | dimensionless heat transfer coefficient for evaporative heating, $h_E v_f^{2/3}/(k_f g^{1/3})$ |
| $h_H^*$ | dimensionless heat transfer coefficient for sensible heating, $h_H v_f^{2/3}/(k_f g^{1/3})$ |
| $k$ | thermal conductivity |
| $L$ | length of heated section |
| $m'$ | mass flow rate per unit film width |
| $P$ | absolute pressure |
| $Pr$ | Prandtl number |
| $Pr_t$ | turbulent Prandtl number |
| $q$ | local wall heat flux |
| $r$ | bubble radius |
| $r_{cav}$ | cavity radius |
| $r_{emb}$ | radius of initial vapor embryo |
| $r_{max}$ | maximum cavity radius |
| $r_{tan}$ | cavity radius based on the tangency criterion for incipience |
| $R_g$ | ideal gas constant |
| $Re$ | film Reynolds number, $4m'/\mu_f$ |
| $T$ | temperature |
| $T_E$ | local temperature based on the Clausius–Clapeyron equation |
| $T_l$ | local liquid temperature |
| $\Delta T_{sat}$ | $T_w - T_{sat}$ |
| $\Delta T_{sub}$ | $T_{sat} - T_{in}$ |
| $v$ | specific volume |
| $v_{fg}$ | specific volume difference, $v_g - v_f$ |
| $x$ | longitudinal distance from the upstream end of the heated section |
| $y$ | distance perpendicular to the heated wall |
| $y_{lam}$ | thickness of laminar sublayer |
| $y_{lam}^+$ | dimensionless thickness of laminar sublayer, $y_{lam}\sqrt{(g\delta)}/v_f$. |

Greek symbols

| | |
|---|---|
| $\Gamma$ | incipience coefficient, $k_f h_{fg}/(8\sigma T_{sat} v_{fg} h_E)$ |
| $\delta$ | mean film thickness |
| $\varepsilon_m$ | eddy momentum diffusivity |
| $\theta$ | contact angle |
| $\mu$ | dynamic viscosity |
| $\nu$ | kinematic viscosity |
| $\sigma$ | surface tension |
| $\phi$ | cavity cone angle |
| $\Psi$ | empirical multiplier, $\Psi_t \Psi_w$ |
| $\Psi_t$ | turbulent boundary layer profile multiplier |
| $\Psi_w$ | wave effect multiplier. |

Subscripts

| | |
|---|---|
| f | liquid |
| g | vapor |
| i | incipience |
| in | inlet |
| m | mean |
| sat | saturation |
| w | wall. |

studies involved a microscopic analysis of the surfaces to confirm this assumption. A summary of previous incipience investigations is given in Table 1.

Recent studies reveal that the onset of nucleate boiling in dielectric fluorocarbon liquids is often accompanied by a severe reduction in wall temperature. Boiling curve hysteresis with distinct boiling incipience and boiling cessation points has been detected in fluorocarbon pool boiling experiments by Bergles and Chyu [21], Marto and Lepere [22] and Moran *et al.* [23]. Similar hysteresis results were also encountered in fluorocarbon flow boiling experiments by Yin and Abdelmessih [16] and Hino and Ueda [17]. Boiling hysteresis was also detected by Hodgson [24] in his water study; however, the severe temperature excursion at ONB observed with fluorocarbon liquids was not encountered with the water experiments. Bar-Cohen and Simon [25] attributed the large temperature excursion associated with boiling of fluorocarbons to the small contact angle of these liquids which allows the liquid to penetrate deep inside surface cavities, resulting in very small vapor embryos. Thus, these cavities require very high wall superheat for incipience. More recently, pool and flow boiling experiments were performed with the dielectric fluorocarbon liquid FC-72 by Anderson and Mudawwar [26] and Maddox and Mudawwar [27], respectively, to better understand parametric influences on hysteresis. They found that the magnitude of the temperature drop at incipience increases with increased soaking time of the surface in the liquid prior to boiling. Owing to the low contact angle of the working fluid, bubbles growing at individual cavities in pool boiling engulfed neighboring cavities with vapor, producing spontaneous nucleation of these surrounding cavities. On the other hand, bubbles growing in a forced liquid stream were pulled from the surface prior to engulfing upstream cavities. Thus, forced convection produced a stabilizing effect against hysteresis by preventing the initial nucleation region from spreading to a larger portion of the heated surface.

This study focuses on predicting boiling incipience in wavy free-falling turbulent liquid films. Exper-

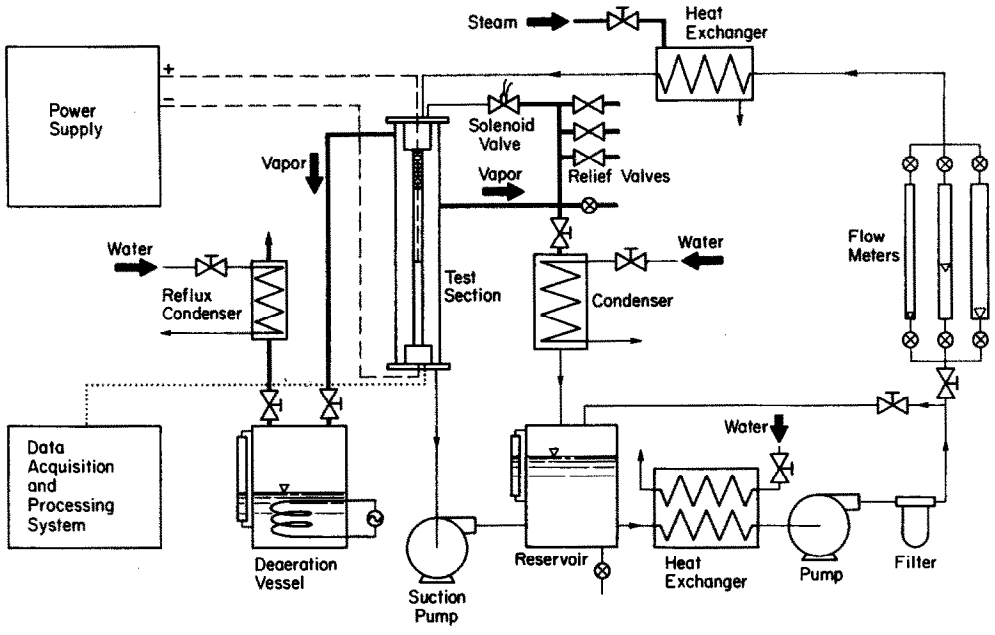


FIG. 1. Schematic diagram of the fluid delivery system.

iments were performed with water and FC-72 films to investigate the effects of interfacial fluid properties on incipience. These two fluids were chosen for this study because of their practical applications (FC-72 is a prime candidate for electronic cooling systems), and because of the significant differences in their physical properties. The surface tension and contact angle of saturated FC-72 at 1 atm are $9.6 \times 10^{-3}$ N $m^{-1}$ (approximately one-sixth that of water) and less than 1°, respectively. In this paper, experimental data from this study are compared to the predictions of existing incipience models to evaluate their applicability to falling film flow, and a new semi-empirical model is used for correlating the effects of waves and turbulent eddies on the onset of nucleate boiling in water films.

## 2. EXPERIMENTAL APPARATUS AND PROCEDURE

The experimental facility utilized in this study has been described in detail in a previous paper by Shmerler and Mudawwar [6]. Only minor changes were necessary to accommodate the use of FC-72 in the present study. A schematic of the modified test facility is shown in Fig. 1. Figure 2 shows a detailed cross-sectional view of the test chamber and sampling scoops used for mean film temperature measurements. The 2.54 cm o.d. vertical cylindrical test section was composed of a polyethylene porous film distributor, a G-10 plastic hydrodynamic development section and a 781 mm long stainless steel heated test section. The stainless steel tube was electrically heated with a low voltage, high d.c. current (up to 15 V at 750 A) to generate uniform heat flux along the direction of fluid flow.

The film heat transfer coefficient was determined by measuring inside wall and mean film temperatures with copper–constantan thermocouples which were calibrated to an accuracy of 0.1°C. The inside wall temperature was measured at 17 locations by thermocouple pairs oriented 180° apart, which allowed for adjustment of the test section to ensure a symmetrical falling film flow. For evaporative heating tests with water, the film temperature at the inlet to the heated test section was maintained at the saturation temperature corresponding to the measured chamber pressure. In the sensible heating tests with FC-72, the mean film temperature was measured at four locations by means of the G-10 fiberglass sampling scoops shown in Fig. 2, and local mean temperatures between scoops were determined from an energy balance based on the measured values.

Each test was initiated by simultaneously circulating and deaerating the fluid within the flow loop. Once deaeration was complete, the inlet temperature was set to the desired subcooling by controlling the steam flow rate through the heat exchanger upstream of the test section, and the heater power was set to a point well below the incipient boiling heat flux. Boiling curves were obtained for each set of inlet conditions by gradually increasing power in small increments while allowing sufficient time for steady-state conditions. As heat flux was increased, boiling incipience was visually monitored and recorded for nucleation sites at each thermocouple. Boiling curve hysteresis

Table 1. Summary of boiling incipience investigations

| Authors [reference] (year) | Flow geometry | Heater material | Fluid | Mean velocity ($m\ s^{-1}$) | Pressure [bar (psia)] | Subcooling (°C) | Incipience formula | Wall temperature excursion at ONB |
|---|---|---|---|---|---|---|---|---|
| Sato and Matsumura [13] (1963) | Vertical channel | Stainless steel | Water | 0.6–4.1 | 1.0 (14.7) | 3–70 | $q_i = \frac{k_f h_{fg}}{8\sigma T_{sat} v_{fg}} (T_{wi} - T_{sat})^2$<br>● tangency criterion, $r = k_f(T_{wi} - T_{sat})/2q_i$ | 0 |
| Bergles and Rohsenow [14] (1964) | Horizontal annulus | Stainless steel | Water | 3.3–17.4 | up to 2.6 (38.0) | 32–90 | $q_i = 15.60p^{1.156}(T_{wi} - T_{sat})^{2.30/p^{0.0234}}$ ($p$ in psia)<br>● graphical solution for water over a pressure range of 15–2000 psia based on the tangency criterion | 0 |
| Han and Griffith [19] (1965) | Pool boiling on a horizontal surface | Gold finished with 600 grit emery paper | Water | —<br>— | 1.0 (14.7) | 7 | $q_i = \frac{k_f h_{fg}}{12\sigma T_{sat} v_{fg}} (T_{wi} - T_{sat})^2$<br>● tangency criterion, $y = 1.5r$ at the point of tangency | 0 |
| Davis and Anderson [15] (1966) | Authors performed analysis using experimental data from prior studies | | | | | | $q_i = \frac{k_f h_{fg}}{C_1 8\sigma T_{sat} v_{fg}} (T_{wi} - T_{sat})^2$<br>● tangency criterion, $y = r$ at the point of tangency<br>● $C_1 = 1$ for hemispherical bubble nucleus | 0 |
| Frost and Dzakowic [20] (1967) | Authors performed analysis using experimental data from prior studies | | | | | | $q_i = \frac{k_f h_{fg}}{8\sigma T_{sat} v_{fg}} (T_{wi} - T_{sat})^2 \frac{1}{Pr_f^2}$<br>● tangency criterion, $y = Pr_f^2 r$ at the point of tangency | 0 |
| Yin and Abdelmessih [16] (1974) | Vertical tube | Stainless steel | Freon 11 | 0.08–0.4 | up to 2.0 (30.0) | 1–20 | ● for increasing heat flux:<br>$q_i = \frac{1}{\left(7 - \frac{q_i}{6500}\right)^2} \frac{k_f h_{fg}}{2\sigma T_{sat} v_{fg}} (T_{wi} - T_{sat})^2$<br>● for decreasing heat flux:<br>$q_i = \frac{k_f h_{fg}}{5\sigma T_{sat} v_{fg}} (T_{wi} - T_{sat})^2$<br>● tangency criterion, $y/r$ at the point of tangency correlated empirically | up to 20 K |

| | | | | | | | | |
|---|---|---|---|---|---|---|---|---|
| Hino and Ueda [17] (1985) | Vertical annulus | Stainless steel finished with 4/0 emery cloth | Freon 113 | 0.1–1.0 | 1.47 (22.0) | 10–30 | • for $r_{tan} < r_{max}$: $q_i = \frac{k_f h_{fg}}{8\sigma T_{sat} v_{fg}} (T_{wi} - T_{sat})^2$ • for $r_{tan} > r_{max}$: $q_i = \frac{k_f}{r_{max}} (T_{wi} - T_{sat}) - \frac{2\sigma T_{sat} v_{fg} k_f}{h_{fg} r_{max}^2}$ | up to 20 K |
| Cerza and Sernas [12] (1985) | Falling film over vertical cylinder | Brass | Water | 0.32–1.03 | 1.0 (14.7) | 0 | • numerical solution for boiling incipience in laminar developing films based on the tangency criterion | 0 |
| Sudo *et al.* [18] (1986) | Vertical channel | Inconel 600 | Water | 0.7–1.5 | 1.2 (17.0) | 28 35 | • for $r_{tan} < r_{max}$: $q_i = \frac{k_f h_{fg}}{8\sigma T_{sat} v_{fg}} (T_{wi} - T_{sat})^2$ • for $r_{tan} > r_{max}$: $q_i = \frac{k_f}{r_{max}} (T_{wi} - T_{sat}) - \frac{2\sigma T_{sat} v_{fg} k_f}{h_{fg} r_{max}^2}$ | up to 2 K |
| Marsh and Mudawar (present study) | Falling film over vertical cylinder | Stainless steel finished with 600 grit paper | Water<br>FC-72 | 1.29–1.79<br>1.03–1.65 | 0.7 (10.2)<br>1.05 (15.0) | 0<br>9–21 | $q_i = \frac{1}{3.5} \frac{k_f h_{fg}}{8\sigma T_{sat} v_{fg}} (T_{wi} - T_{sat})^2$ • modified tangency criterion which accounts for turbulence and waviness in water films • the correlation does not apply for highly wetting fluids | 0 |

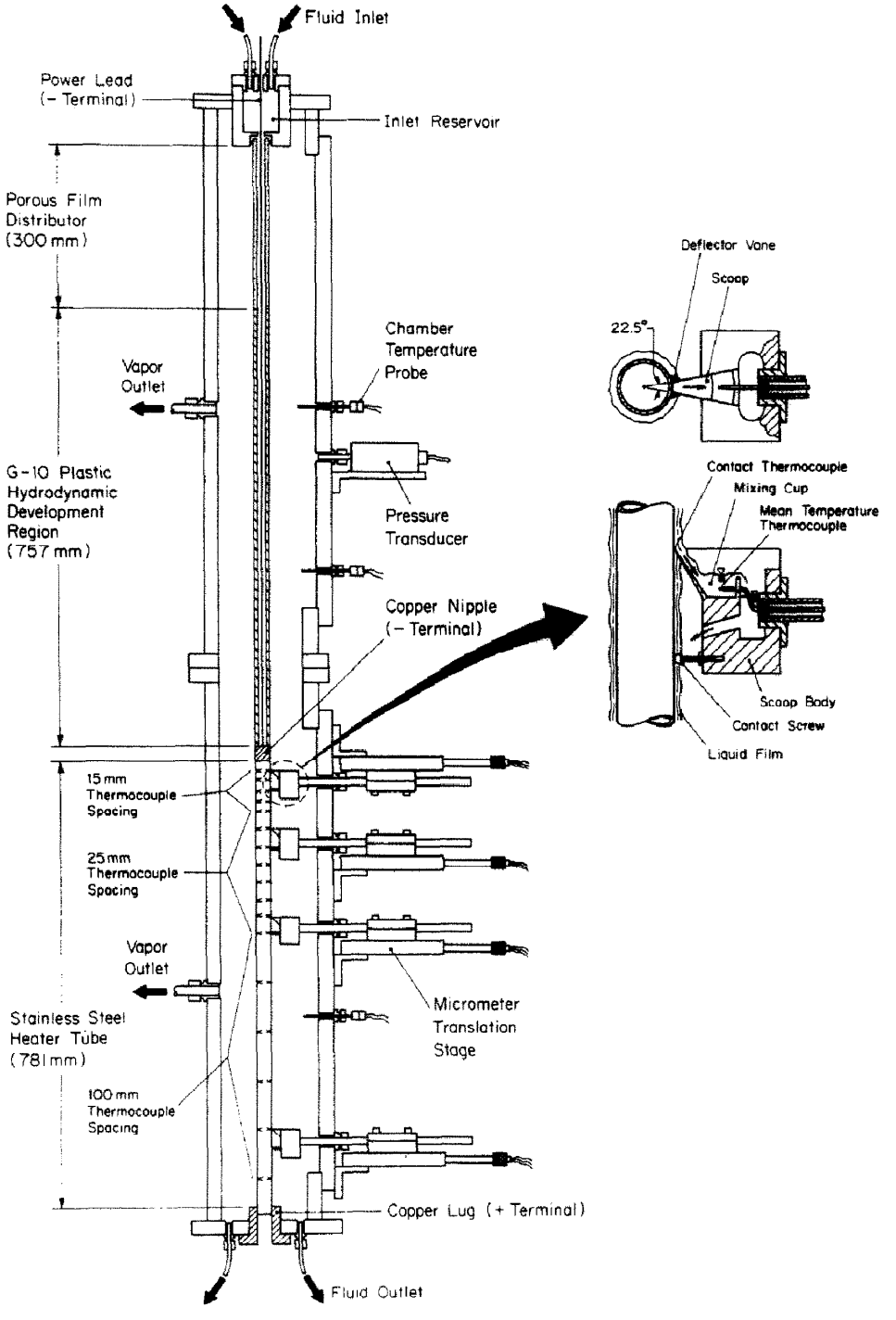


FIG. 2. Cross-sectional diagram of the test chamber and sampling scoops.

was investigated by increasing the heat flux to a point of fully developed nucleate boiling to remove air from surface cavities, followed by decreasing the heat flux to a point well below boiling cessation. After a 2 h waiting period, the heat flux was again increased to measure any wall temperature excursions at incipient boiling.

## 3. EXPERIMENTAL RESULTS AND DISCUSSION

Experiments were performed with FC-72 and water films subjected, respectively, to sensible heating and interfacial evaporation prior to incipient boiling. The ranges of operating conditions for each fluid are sum-

Table 2. Operating conditions of the present study

| Fluid | Pressure bar (psia) | Degree of subcooling (°C) | $Re \times 10^{-3}$ | $Pr_f$ |
|---|---|---|---|---|
| water | 0.7 (10.2) | 0 | 11–24 | 1.95 |
| FC-72 | 1.05 (15.0) | 6–21 | 7–23 | 9.75–10.75 |

marized in Table 2. These studies were performed in an effort to predict the incipient wall heat flux and incipient superheat by relating each of these parameters independently to the convective heat transfer coefficient just prior to boiling.

Figure 3 shows the variation of wall temperature as a function of position along the heated length for water and for FC-72. The water evaporation data are characterized by fairly constant wall temperature followed by a reduction in wall temperature beyond the onset of nucleation. The FC-72 sensible heating data indicate a fairly uniform temperature increase in the single phase region followed by a leveling off or slight decrease in temperature upon reaching boiling incipience. Similar plots by Yin and Abdelmessih [16] and Hino and Ueda [17] showed temperature drops of as much as 20°C at ONB for their fluorocarbon forced convection data. As indicated in Fig. 3, these types of temperature drops were nonexistent in the present study.

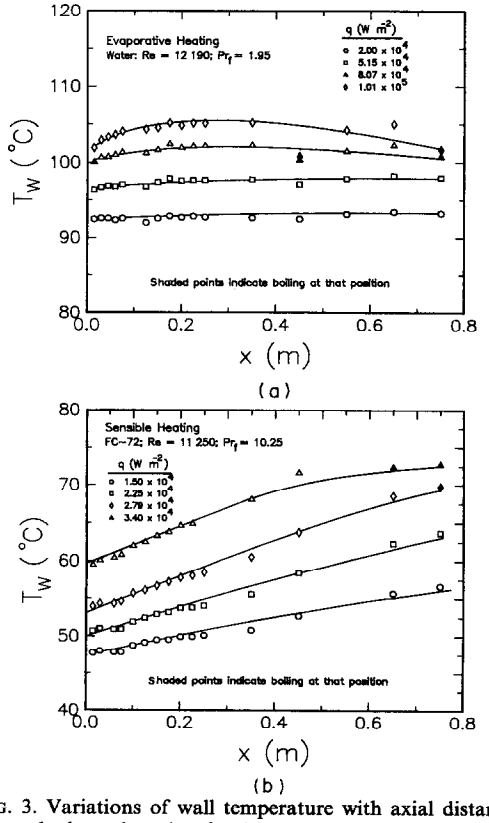


FIG. 3. Variations of wall temperature with axial distance along the heated section for (a) water evaporation and (b) FC-72 sensible heating.

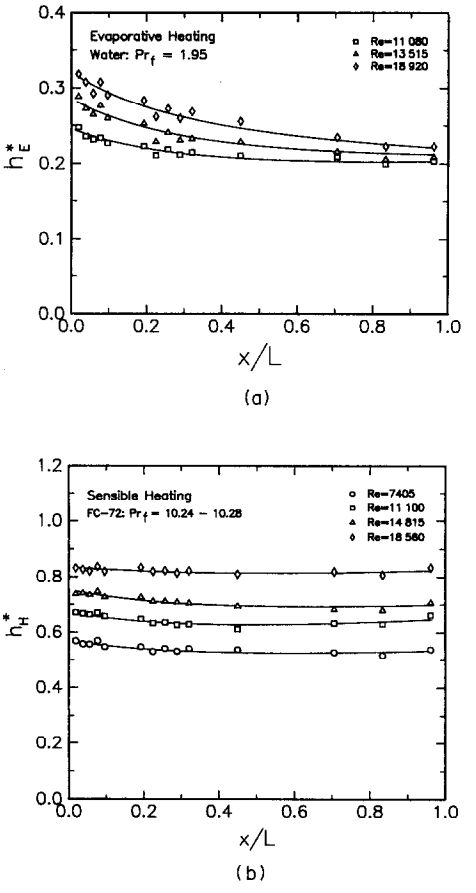


FIG. 4. Variations of the dimensionless heat transfer coefficient with distance along the heated section for (a) water evaporation and (b) FC-72 sensible heating.

### 3.1. *Sensible and evaporative heating*

Figure 4 shows variations of the dimensionless heat transfer coefficients $h_E^*$ and $h_H^*$ for representative water evaporative heating data and FC-72 sensible heating data with the dimensionless length $x/L$, where $L$ is the length of the electrically heated test section. The fluid properties used to nondimensionalize $h_E^*$ and the reference Reynolds and Prandtl numbers for evaporation tests are evaluated at the saturation temperature. In the sensible heating tests, fluid properties in $h_H^*$ are evaluated at the local measured mean film temperature, and the reference Reynolds and Prandtl numbers are evaluated at the fluid inlet temperature.

As shown in Fig. 4(a), the dimensionless evaporative heat transfer coefficient $h_E^*$ exhibits a thermal development region persisting over more than half of the heated section. Shmerler and Mudawwar [9] attributed this effect to a thermal boundary layer forming at the film interface and predicted the development of this layer using semi-empirical turbulent film models. They demonstrated the existence of two major sources of thermal resistance across thin films: a boundary layer forming at the wall, and a second resistance associated with interfacial damping at the film interface. The development region associated with interfacial resistance was very long in the case of

evaporating films and nonexistent in films subjected to sensible heating due to the negligible heat flux at the interface of heated films. The wall boundary layer, on the other hand, displayed rapid development over a short distance from the entrance to the heated section for both heated and evaporating films.

The dimensionless sensible heat transfer coefficient for the present FC-72 data, Fig. 4(b), exhibits only a gradual decrease at the upstream positions, indicating rapid development of the wall thermal boundary layer upstream of the first thermocouple position. The decrease in $h_H^*$ continued until approximately the middle of the heated length, at which point $h_H^*$ gradually increased or reached an asymptotic value. Shmerler and Mudawwar [6, 9] postulated that increased waviness in a falling film was responsible for the downstream enhancement in the heat transfer coefficient. In comparison to Shmerler and Mudawwar's [6] water heating data, downstream enhancement in $h_H^*$ for FC-72 was very slight. During experimental runs it was observed that a significant amount of liquid splashed away from the FC-72 film interface. This splashing significantly increased film thickness and reduced film flow rate which was, perhaps, responsible for the decreased downstream enhancement when compared to water data. The low surface tension of FC-72 seems to have induced the severe splashing. A visually observed increase in downstream splashing at higher inlet temperatures (i.e. lower surface tension) further substantiates this conclusion. Fluid splashing was most severe during preliminary experiments involving evaporative heating of FC-72 films at atmospheric pressure. These experiments had to be aborted to prevent dryout from occurring at the downstream end of the heater.

A space-averaged dimensionless heat transfer coefficient was determined for both water and FC-72 using temperature measurements obtained by the four thermocouples upstream of the last thermocouple position. Figure 5 shows log–log regression curve fits of the present data along with Shmerler and Mudawwar's correlations for sensible and evaporative heating of water films. The evaporative heating water data in the present experiment were consistent with Shmerler and Mudawwar's [9] correlation as shown in Fig. 5(a). Figure 5(b) displays noticeable differences between water and FC-72 sensible heating correlations. These differences can be attributed to the surface tension effects discussed earlier since the greater amount of downstream enhancement in Shmerler and Mudawwar's water tests increased the average of the downstream data points. The average heat transfer coefficient for FC-72 was correlated as

$$h_H^* = 0.0022 Re^{0.45} Pr_f^{0.63}. \quad (1)$$

This correlation has an average error of 1.6% with a maximum error and standard deviation of 4.4% and 0.165, respectively. Due to lack of understanding of the influence of surface tension of $h_H$ in FC-72 films, equation (1) should be treated as an empirical correlation which is valid only for the conditions of the present study.

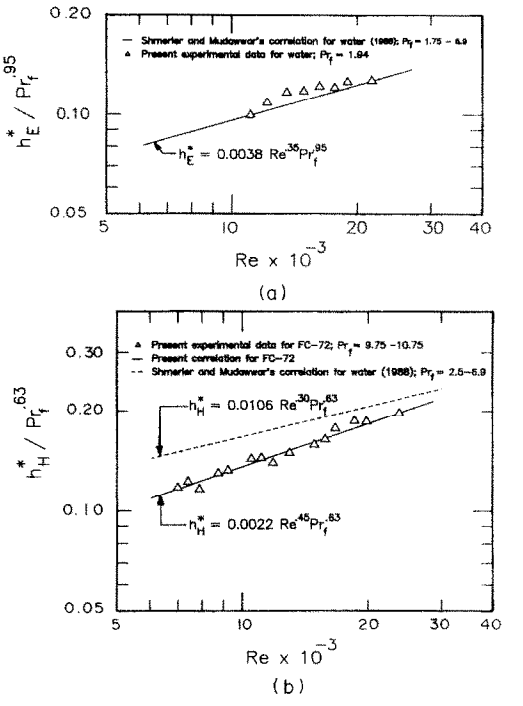


FIG. 5. Correlations for the space-averaged dimensionless heat transfer coefficient with Reynolds number for (a) water evaporation and (b) FC-72 sensible heating.

### 3.2. *Boiling incipience*

Figure 6 shows boiling curves for representative experiments with saturated water and subcooled FC-72. Visually observed boiling incipience is indicated by an arrow on each curve and is usually followed by a rapid increase in the heat transfer coefficient. The slopes in the forced convection single-phase region for water and FC-72 are different because of subcooling in the FC-72 tests.

Many of the FC-72 single phase and boiling phenomena described in this paper were investigated with the aid of still photography. It was observed that waviness and breakup of liquid droplets from the film interface occurred both prior to and after incipience. Figure 7 shows photographs obtained during an FC-72 data run with a Reynolds number of 11 100 and 20 K subcooling. These photographs were taken at increasing levels of heat flux to identify the role of interfacial waves on the development of film flow in the single phase and boiling regions. The non-boiling flow shown in Fig. 7(a) is characterized by large waves separated by regions of thin, less disturbed film motion. Some interfacial breakup of droplets at wave crests is also visible. Droplet formation was more pronounced in FC-72 films compared to water films due to the low surface tension of FC-72. Boiling incipience sites and downstream boiling streamers are shown in Fig. 7(b). Figures 7(c) and (d) show fully developed nucleate boiling with significant splashing

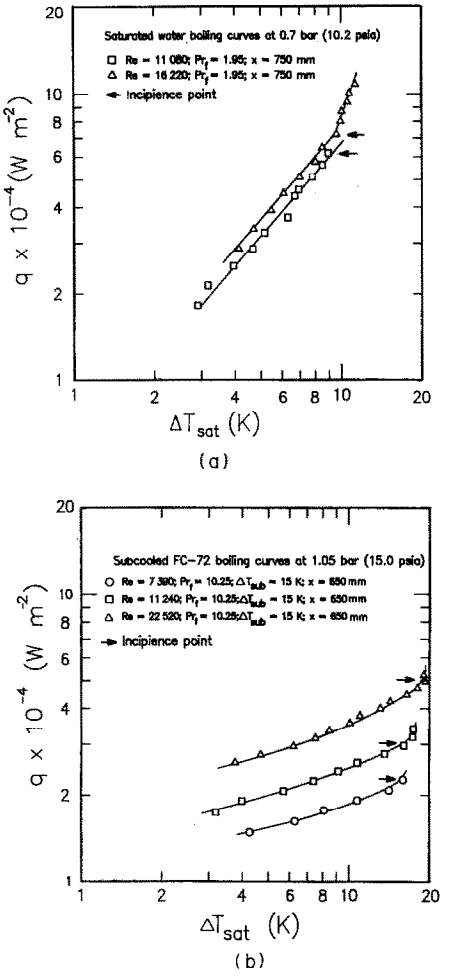


FIG. 6. Boiling curves for (a) saturated water and (b) subcooled FC-72.

induced by boiling. This form of splashing occurred both in FC-72 and water films and is attributed to the inability of thin films to maintain a liquid continuum against the significant increase in void fraction in the direction of film flow. Figure 7(c) also shows that large waves induce significant boiling in the film, while the region of thin film flow between the large waves suppresses nucleation. Figure 7(d) depicts a boiling wave front and a partial dryout region which was a precursor for critical heat flux at the downstream end of the heated section.

The photographs shown in Fig. 7 make it obvious that interfacial disturbances in a falling film add significant difficulty to any numerical prediction of the single phase heat transfer coefficient and especially boiling incipience. Figure 7(c) provides strong evidence that falling film incipience models should take into direct account the effect of wave fronts on transient heating and cooling of the solid wall. These observations were also evident in water experiments except for the reduced level of fluid splashing in the case of water compared to FC-72.

The majority of the previous studies on boiling incipience have used water as the working fluid. Early forced convection incipience studies, Table 1, predicted incipience for cases where a wide range of cavity sizes existed on the heated surface. A popular incipience equation based on this theory [13, 15] is

$$q_i = \frac{k_f h_{fg}}{8\sigma T_{sat} v_{fg}} (T_{wi} - T_{sat})^2. \quad (2)$$

Equation (2) is based on the assumption that a bubble will grow beyond the mouth of a cavity when its entire surface is sufficiently superheated to maintain stable mechanical equilibrium at the vapor–liquid interface. As shown schematically in Fig. 8(a) (modified representation of incipience based on ref. [14]), the incipience condition for equation (2) is determined by the tangency point, $y = r_{tan}$, between the liquid temperature profile, $T_{l1}$, and the excess (Clapeyron) superheat profile, $T_E$. Equation (2) is also based on the assumption that $r_{tan}$ is less than the superheated sublayer thickness, $y_{lam}$. Yin and Abdelmessih [16] used a similar tangency assumption, but they extended the analysis to obtain an equation for $\delta^*/r_{tan}$, where $\delta^*$ is the thickness of the superheated liquid layer near the wall. Solving empirically for $\delta^*/r_{tan}$, they obtained two incipience equations—one for increasing heat flux and the other for decreasing heat flux.

Cerza and Sernas [11] noted that a bubble may still grow at $y = r_{tan}$ and $T_l < T_E$ if there was a net positive incoming heat flux over the bubble surface. This statement was made in conjunction with Han and Griffith's [19] argument that an isotherm must dip slightly in the vicinity of the bubble cap to allow for heat transfer to the bubble interface, thereby causing $y > r_{tan}$. Cerza and Sernas combined the Clapeyron criterion with a laminar entry length liquid temperature profile rather than assuming a linear liquid temperature profile in the laminar sublayer region. Their analysis was performed to determine a range of permissible active nucleation site radii and to determine if these radii compare favorably to the standard pool boiling incipience (Clapeyron) criterion. Their conclusion was that the Clapeyron criterion is valid for thin films, but their analysis did not include comparisons to previous correlations for boiling incipience or predictions for turbulent wavy film flow.

A second commonly accepted incipience equation applies to conditions where the calculated radius for the first active cavity, $r_{tan}$, exceeds the maximum available cavity radius $r_{max}$. This case is shown in Fig. 8(b) and incipience is postulated to occur when the liquid temperature $T_{l2}$ equals the required superheat $T_E$ at $y = r_{max}$. The incipience equation resulting from these assumptions is

$$q_i = \frac{k_f}{r_{max}} (T_{wi} - T_{sat}) - \frac{2\sigma T_{sat} v_{fg} k_f}{h_{fg} r_{max}^2}. \quad (3)$$

Equation (3) has been used by Hino and Ueda [17] and Sudo *et al.* [18] in their analyses of incipience data. This equation is most useful for very smooth

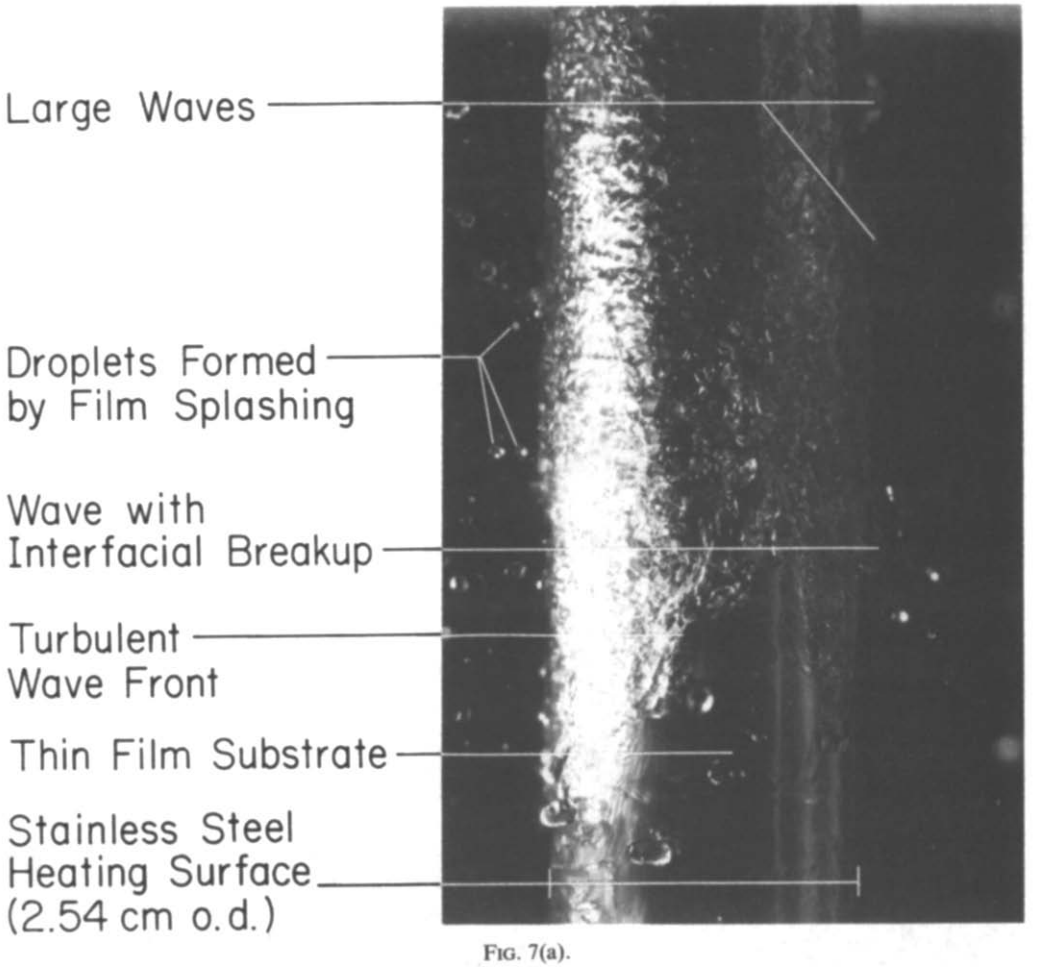


FIG. 7(a).

surfaces where the maximum cavity radius tends to be smaller than $r_{tan}$.

Incipience conditions for water and FC-72 obtained in this study are shown in Fig. 9. Saturated water data obtained at thermocouple positions $x = 125$ and 450 mm are plotted for a range of Reynolds numbers. FC-72 incipience conditions at thermocouple position $x = 650$ mm are shown in Fig. 9(b) for three levels of subcooling and a range of Reynolds numbers. Figures 9(a) and (b) also display lines representing equations (2) and (3). It is obvious from these two figures that incipience conditions differ markedly for the two fluids. The water data in Fig. 9(a) follow the trend of equation (2), yet there is up to 4 K or 50% error between the actual and predicted values based on the tangency criterion. The poor agreement between experimental data and the theoretical prediction is evidence of the unique nature of the incipience phenomenon in falling films. In any case, the trend of increased superheat and heat flux at ONB for higher flow rates is evident. Previous incipience studies with water [13–15, 18] reported similar trends for boiling incipience.

3.2.1. *Incipience in water films.* Because equation (2) was based on the assumption that the liquid temperature profile is linear in the laminar sublayer, it is important to determine the laminar sublayer thickness, $y_{lam}$, in comparison to the tangency radius $r_{tan}$. The laminar sublayer thickness can be calculated from

$$y^+_{lam} = \frac{y_{lam}\sqrt{(g\delta)}}{\nu_f} = 5 \tag{4}$$

where $\delta$ is the film thickness obtained from the empirical correlation by Gimbutis *et al.* [3]

$$\delta = 0.136\left(\frac{\nu_f^2}{g}\right)^{1/3} Re^{0.583}. \tag{5}$$

Figure 10 shows a comparison of the laminar sublayer thickness and the present $r_{tan}$ data based on the following equation [15]:

$$r_{tan} = \sqrt{\left(\frac{2\sigma T_{sat}\nu_{fg}k_f}{h_{fg}q_i}\right)}. \tag{6}$$

The result $r_{tan} > y_{lam}$ is strong evidence that the linear liquid temperature profile assumption of equation (2) is not valid for the present falling film data. This result is very significant because it would partially explain the error between actual and predicted water incipience results.

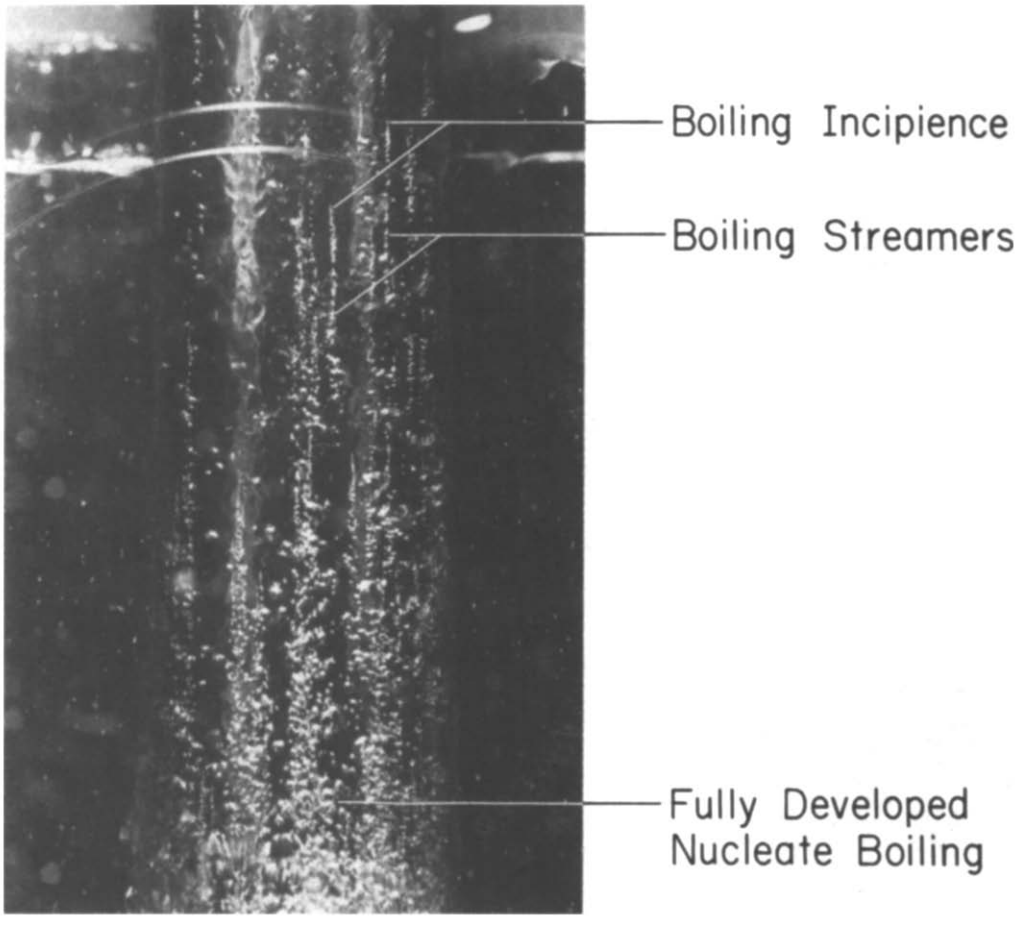


FIG. 7(b).

Rather than assuming a linear temperature profile in the laminar sublayer region, a turbulent film temperature profile may be employed. Assuming a constant wall flux, the temperature gradient and mean liquid temperature in the turbulent boundary layer are given by

$$\frac{dT_l}{dy} = -\frac{q}{k_f}\frac{1}{\left[1+\frac{Pr_f}{Pr_t}\frac{\varepsilon_m}{\nu_f}\right]} \tag{7}$$

$$T_l = T_w - \frac{q}{k_f}\int_0^y \frac{1}{\left[1+\frac{Pr_f}{Pr_t}\frac{\varepsilon_m}{\nu_f}\right]}dy. \tag{8}$$

The equation for the superheated vapor temperature profile $T_E$ can be obtained from the Clausius–Clapeyron relation assuming a constant value for $Tv_{fg}/h_{fg}$ within the wall superheat range associated with incipience. This assumption yields

$$T_E = T_{sat} + \frac{T_{sat}v_{fg}}{h_{fg}}\frac{2\sigma}{r}. \tag{9}$$

The radius of the first cavity at which boiling occurs can be determined by equating the slopes of $T_l$ and $T_E$. That is

$$\frac{dT_l}{dy} = \frac{dT_E}{dr} \tag{10}$$

or

$$r_{tan} = \left[\frac{2\sigma T_{sat}v_{fg}k_f}{h_{fg}q_i}\right]^{1/2}\left[1+\frac{Pr_f}{Pr_t}\frac{\varepsilon_m}{\nu_f}\bigg|_{r_{tan}}\right]^{1/2}. \tag{11}$$

Equation (11) for the tangency radius is similar to equation (6) except for the turbulent eddy diffusivity term. From equation (11) it is clear that $r_{tan}$ will be greater for turbulent films than predicted by equation (6) because

$$\left[1+\frac{Pr_f}{Pr_t}\frac{\varepsilon_m}{\nu_f}\bigg|_{r_{tan}}\right]^{1/2} \geqslant 1. \tag{12}$$

In addition to their slopes being equal, the temperatures $T_E$ and $T_l$ must also be equal at the point of tangency. Equating equations (8) and (9) results in

$$T_{wi} - T_{sat} = \frac{q_i r_{tan}}{k_f}\int_0^1 \frac{1}{\left[1+\frac{Pr_f}{Pr_t}\frac{\varepsilon_m}{\nu_f}\right]}d\left(\frac{y}{r_{tan}}\right) + \frac{T_{sat}v_{fg}}{h_{fg}}\frac{2\sigma}{r_{tan}}. \tag{13}$$

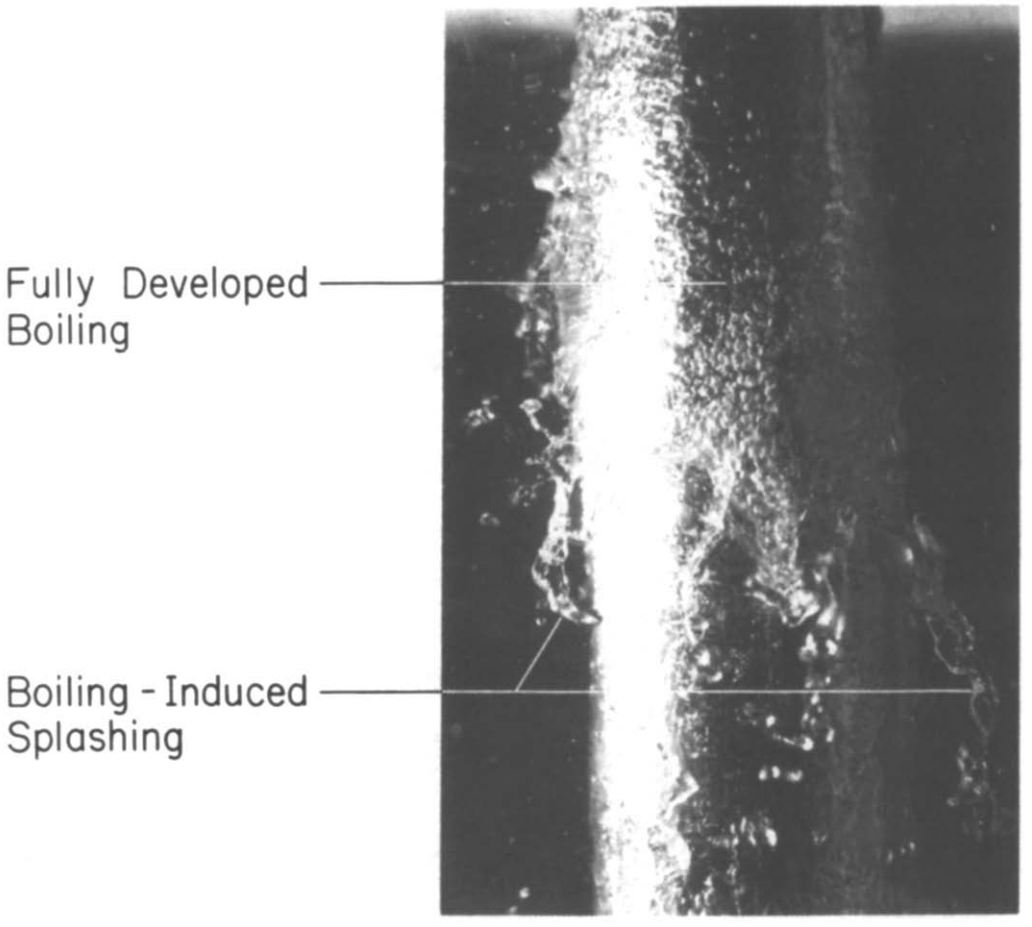


FIG. 7(c).

Substituting equation (11) for $r_{tan}$ in equation (13) yields

$$T_{wi} - T_{sat} = \left[\frac{8\sigma T_{sat} v_{fg} q_i}{h_{fg} k_f}\right]^{1/2} \Psi_t^{1/2}. \quad (14)$$

The turbulent boundary layer profile multiplier is defined as

$$\Psi_t = \frac{\left[\frac{1}{2} + \frac{1}{2}\int_0^1 \frac{\left[1 + \frac{Pr_f}{Pr_t}\frac{\varepsilon_m}{\nu_f}\Big|_{r_{tan}}\right]}{\left[1 + \frac{Pr_f}{Pr_t}\frac{\varepsilon_m}{\nu_f}\right]} d\left(\frac{y}{r_{tan}}\right)\right]^2}{\left[1 + \frac{Pr_f}{Pr_t}\frac{\varepsilon_m}{\nu_f}\Big|_{r_{tan}}\right]}. \quad (15)$$

Equation (14) is a more general expression for incipience in turbulent boundary layers including flow in closed channels. However, it does not account for the curvature of isotherms around growing bubbles. Furthermore, equation (14) assumes bubble growth based on the mean fluid temperature within the turbulent boundary layer. Turbulent eddies, however, may have a strong influence in suppressing the growth of bubbles at potential nucleation sites via cold fluid continuously supplied from the film to the wall. This may happen despite the high mean liquid superheat available at the wall. These transient phenomena create a quenching effect on the nucleation process which is furthermore complicated by interfacial waves. The periodicity of turbulent bursts at the wall is continuously interrupted by the passage of waves which are characterized by a very complex flow pattern. During nucleate boiling, a larger wall superheat is created upon the passage of large waves, providing more favorable conditions for nucleation compared to the thin film between the large waves. At the point of incipience, wall regions which are instantaneously favorable for bubble growth due to the passage of large waves are quickly covered with thin film flow, which, together with the turbulent eddies, tend to deprive wall cavities of the superheat required for nucleation. The authors postulate that these effects dominate the process of nucleation in falling films, creating the need for empirical modeling of incipience based on experimental results.

In addition to the turbulent boundary layer effect,

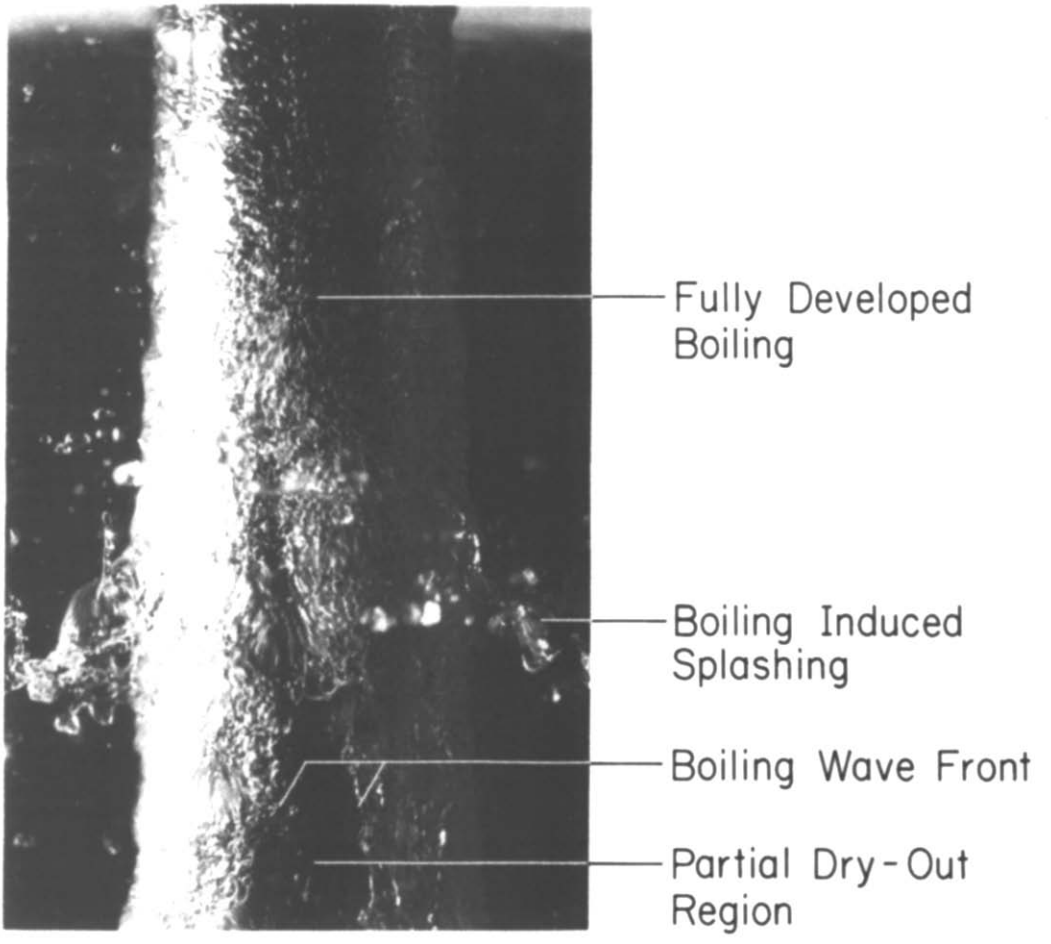


FIG. 7. Photographs of FC-72 film flow at $Re = 11\,100$, $\Delta T_{sub} = 20$ K and increasing levels of heat flux. (a) Single phase film flow, $q = 0$ W m$^{-2}$. (b) Boiling incipience, $q = 3.0 \times 10^4$ W m$^{-2}$. (c) Fully developed boiling, $q = 3.9 \times 10^4$ W m$^{-2}$. (d) Fully developed boiling, $q = 4.4 \times 10^4$ W m$^{-2}$.

the effects of waves, turbulent eddies, and isotherm curvature in a falling film can be modeled by another coefficient $\Psi_w^{1/2}$. That is

$$T_{wi} - T_{sat} = \left[\frac{8\sigma T_{sat} v_{fg} q_i}{h_{fg} k_f}\right]^{1/2} \Psi_t^{1/2} \Psi_w^{1/2}. \quad (16)$$

Rearranging equation (16) gives the heat flux

$$q_i = \frac{k_f h_{fg}}{8\sigma T_{sat} v_{fg}} (T_{wi} - T_{sat})^2 \frac{1}{\Psi} \quad (17)$$

where

$$\Psi \equiv \Psi_t \Psi_w. \quad (18)$$

Equation (17) is very similar to equation (2) except for the combined film multiplier, $\Psi$. A least squares approximation to the water incipience data shown in Fig. 9(a) gives an empirical value of $\Psi = 3.5$ with a mean error of 5.2%. The relatively large value of $\Psi$ can be explained by the pronounced waviness of film flow, causing instantaneous film thickness variations of as much as 250% above and 50% below the mean thickness [6].

An alternative method to determining $\Psi$ can be employed if the heat transfer coefficient is known. In addition to equation (17), the heat flux at incipience for saturated films is related to the evaporative heat transfer coefficient by

$$q_i = h_E (T_{wi} - T_{sat}). \quad (19)$$

Combining equations (16) and (19), the incipient wall superheat and heat flux become

$$(T_{wi} - T_{sat}) = \frac{1}{\Gamma} \Psi \quad (20)$$

$$q_i = \frac{h_E}{\Gamma} \Psi \quad (21)$$

where

$$\Gamma \equiv \frac{k_f h_{fg}}{8\sigma T_{sat} v_{fg} h_E}. \quad (22)$$

The value of $\Gamma$ can be determined by employing Shmerler and Mudawwar's [9] equation for the evaporative heat transfer coefficient provided in Fig. 5(a).

Figure 11 shows a comparison of present water incipience data and predictions based on equations (2) and (17). Also shown in Fig. 11 is an equation

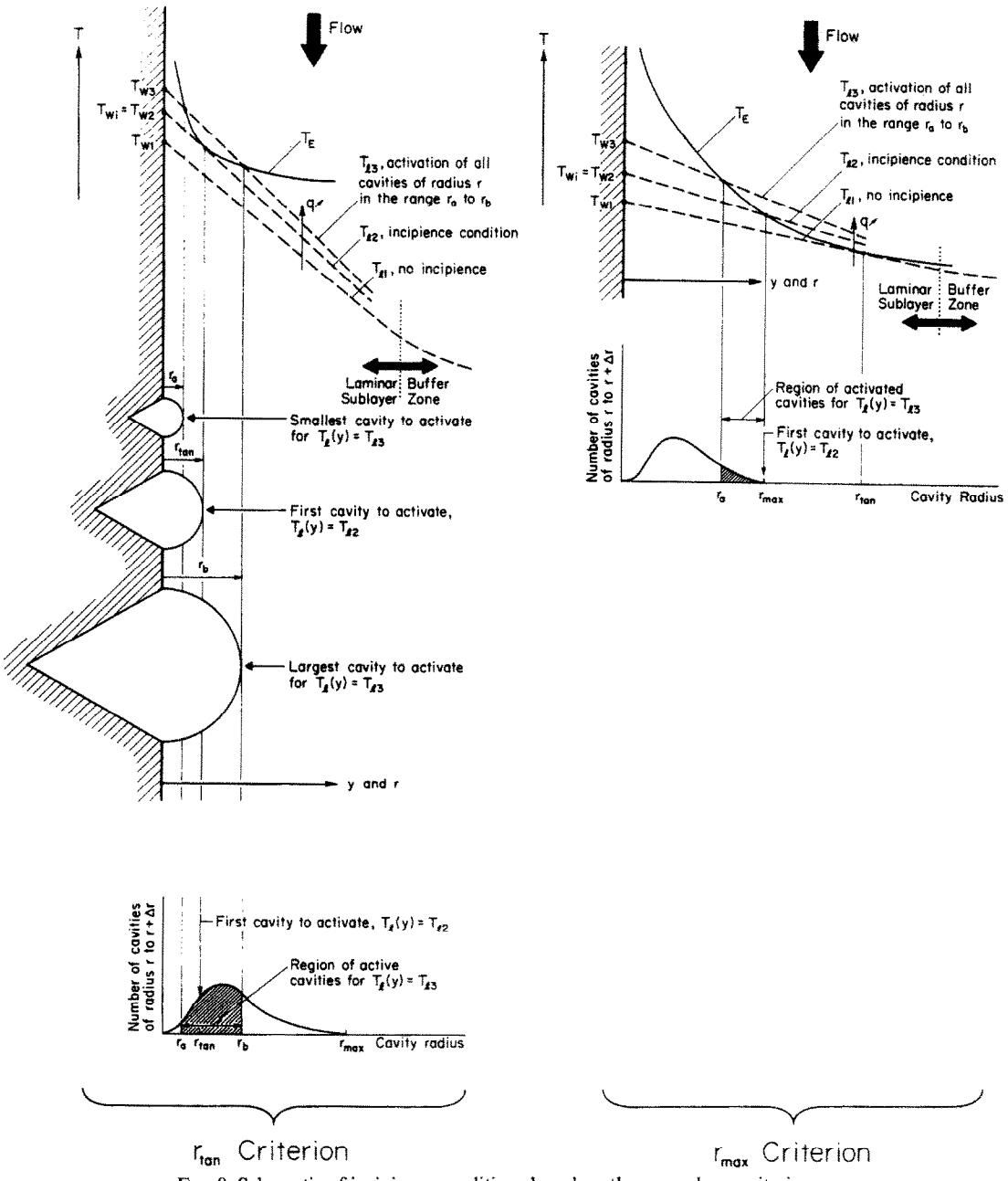


FIG. 8. Schematic of incipience conditions based on the $r_{tan}$ and $r_{max}$ criteria.

developed by Frost and Dzakowic [20] which was given in the form

$$q_i = \frac{k_f h_{fg}}{8\sigma T_{sat} v_{fg}} (T_{wi} - T_{sat})^2 \frac{1}{Pr_f^2}. \quad (23)$$

Equation (23) was developed with the assumption that nucleation occurs at a surface when the liquid temperature $T_l(y)$ just exceeds the vapor bubble temperature $T_E$ at a distance $y = Pr_f^2 r_{tan}$; but no detailed physical explanation was provided for this assumption. Nevertheless, equation (23) has been fairly successful in correlating incipience data for a large number of fluids. Figure 11 shows good agreement between the present correlation for falling films and equation (23), and a significant departure from equation (2). It is difficult to conclude at this point that the agreement between the closed channel flow and falling film correlations is predominantly due to turbulent eddies and not to wave-induced effects.

3.2.2. *Incipience in* FC-72 *films.* As shown in Fig. 9(a), incipient superheat and heat flux for water increase with flow rate and subcooling, yet this is not the case with FC-72. The wall superheat at ONB in FC-72 appears to be independent of subcooling or flow

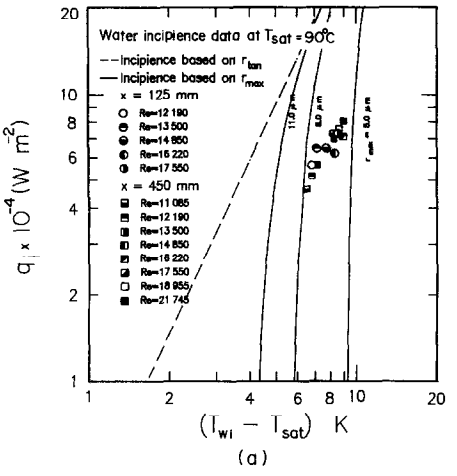


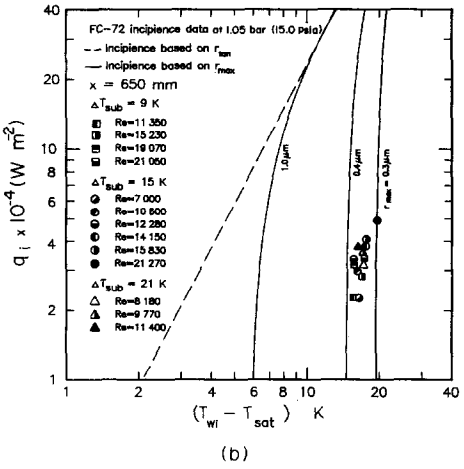


FIG. 9. Comparison of present incipience data for (a) water and (b) FC-72 with incipience models based on the $r_{tan}$ and $r_{max}$ criteria (equations (2) and (3), respectively).

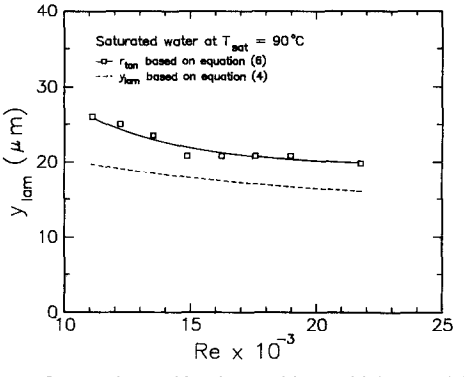


FIG. 10. Comparison of laminar sublayer thickness with $r_{tan}$ for the present water data.

rate. The data of Fig. 9(b) also indicate that $r_{max}$ for FC-72 films ranges from 0.30 to 0.40 μm. Hino and Ueda [17] presented similar trends for R-113 forced convection experiments with $r_{max}$ ranging from 0.22 to 0.34 μm based on equation (3), and with velocity and subcooling having negligible effect on the incipient superheat. They concluded that the maximum cavity radius on their heat transfer surface must be within that range without conducting a physical inspection of the surface.

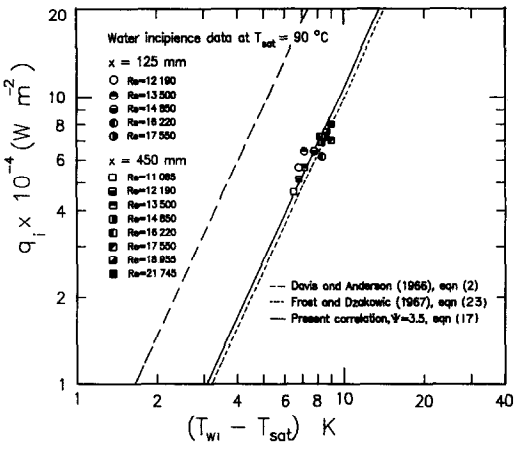


FIG. 11. Correlation for water incipience data.

In order to determine the validity of the $r_{max}$ correlation for the present FC-72 data, a microscopic evaluation of the heat transfer surface was performed. Microscopic photographs showed pits or cavities as large as 50 μm in radius that could not be removed by polishing, and a large population of surface cavities ranging from 0.5 to 10 μm. It should be emphasized that microscopic photographs of the heated surface may not necessarily provide information on the inner shape or effective diameters of the cavities. Nevertheless, the availability of outer cavity radii as large as 50 μm clearly contradicts the $r_{max}$ range of 0.3–0.4 μm predicted by equation (3). Therefore, the authors conclude that equation (3) is invalid in predicting incipience in FC-72 falling films. Also, because ONB in FC-72 appears to be independent of subcooling or flow rate, it is believed that the incipience superheat for highly wetting fluids is determined solely by the initial radius of the trapped vapor embryo rather than the temperature distribution in the fluid outside the cavity. This is a result of deep penetration of the liquid front inside surface cavities, which leaves a relatively small vapor embryo within the heated surface. The radius of the initial vapor embryo depends on the shape, size, and cone angle ($\phi$) of the cavity, and the wetting angle, $\theta$, of the fluid with the surface. Lorenz *et al.* [28] predicted ratios of $r_{emb}/r_{cav}$ for a range of cavity sizes and fluid wetting angles. They determined that for highly wetting fluids (small $\theta$) the surface acts as though it had smaller cavities than what actually existed, requiring higher superheat for incipience. The plots of $r_{emb}/r_{cav}$ by Lorenz *et al.* would be useful for fluids with wetting angles greater than 10°, but the small wetting angle of FC-72 negates the usefulness of these plots.

Because the minimum superheat required for incipience of highly wetting fluids is dependent upon the initial vapor embryo radius and not cavity radius, the

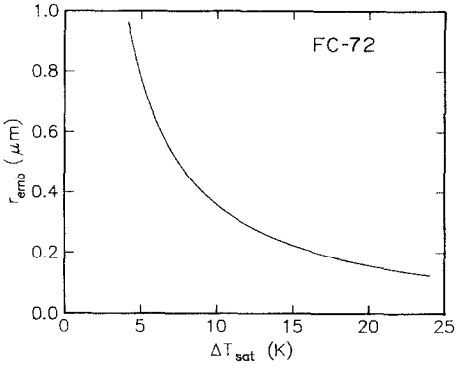


FIG. 12. Variation of predicted vapor embryo radius as a function of wall superheat for FC-72.

wall superheat can be determined by direct integration of the Clausius–Clapeyron relation. Mechanical equilibrium at the liquid–vapor interface requires that

$$P_g - P_f = \frac{2\sigma}{r}. \tag{24}$$

The Clausius–Clapeyron relation

$$\frac{dT}{dP} = \frac{Tv_{fg}}{h_{fg}} \tag{25}$$

can be integrated in the form

$$\int_{P_f}^{P_f + 2\sigma/r} dP = \int_{T_{sat}}^{T_{wi}} \frac{h_{fg}}{v_{fg}} \frac{dT}{T}. \tag{26}$$

Combining equations (24) and (26) yields the relation

$$r_{emb} = \frac{2\sigma}{\int_{T_{sat}}^{T_{wi}} \frac{h_{fg}}{v_{fg}} \frac{dT}{T}}. \tag{27}$$

Figure 12 shows a numerical integration of equation (27) based on tabulated property values of FC-72. For a wall superheat of 15 K, an embryo radius of 0.224 $\mu$m is expected. This value is an order of magnitude lower than the typical cavity radii detected in the microscopic photographs, which confirms earlier arguments on the ability of wetting liquids to penetrate inside surface cavities. Unfortunately, it is impossible to confirm the numerical predictions of equation (27) for the present data or the data of previous studies involving highly wetting fluids in the absence of reliable microscopic measurements of $r_{emb}$.

The present incipience analysis for water and FC-72 falling films has shown important differences in incipience conditions. Water data followed the trend of equation (2) which had to be corrected for turbulence and wave effects, while FC-72 data were inconsistent with equations (2) and (3). Also, water nucleation sites started boiling at large surface pits and cavities and FC-72 nucleation sites began from within much smaller cavities. Figure 13 shows a possible explanation for these differences. Two cases of bubble growth are shown: the first is for a fluid such as water with $\theta \approx 90°$, and the second is for a highly wetting fluid such as FC-72 with $\theta \to 0°$. The radius of the initial vapor embryo for water would be larger than the cavity. Since the wall superheat is inversely proportional to bubble radius, the wall superheat required to initiate nucleate boiling is determined by the smallest bubble radius near the mouth of the cavity, which in the case of water corresponds to the cavity radius itself. For FC-72, on the other hand, the initial vapor embryo $r_1$ would require greater superheat than that corresponding to $r_{cav}$. This was confirmed in the present study by visual observation of bubbles nucleating randomly at smaller wall cavities instead of originating from larger cavities which were carefully identified at specific locations prior to each experimental run.

The vanishingly small contact angle of dielectric fluids as shown in Fig. 13 has often been described as the major contributor to large temperature excursions at ONB. It has been postulated that when the liquid front of a highly wetting fluid passes over a surface, the cavities would be flooded with liquid, leaving a very small vapor embryo. However, Figs. 3(b) and 6(b) show that the temperature drop commonly encountered in pool or flow boiling dielectric systems [17, 18, 21–23] is nonexistent in the present study. Hysteresis was also absent from the FC-72 falling film data of Mudawwar *et al.* [29] and the R-113 thin wall jet study of Toda and Uchida [30], both of which involved flow boiling with a free liquid interface. Present experiments with increasing followed by decreasing heat flux showed that active nucleation sites in the region between boiling incipience and boiling cessation had little effect on the overall heat transfer coefficient. Thus, for small nucleation site densities on the surface, the forced convection heat transfer coefficient remains the major contributor to the overall flow boiling heat transfer coefficient. This poses a possible explanation for the absence of temperature excursion at ONB in thin films. However, forced convection studies [17, 18] utilizing similar wetting fluids reported temperature excursions up to 20 K. This may indicate that incipience in falling films of wetting fluids may be aided by a fine bubble entrainment mechanism prior to boiling, caused by the fluid churning induced by waves. Boiling in closed channels, however, is solely dependent on vapor trapped within the surface.

## 4. CONCLUSIONS

This study has focused on predicting boiling incipience in free-falling water and FC-72 films. Key conclusions from the study are as follows.

(1) The heat transfer coefficient in falling liquid films prior to, and during nucleate boiling is strongly influenced by the surface tension of the working fluid.

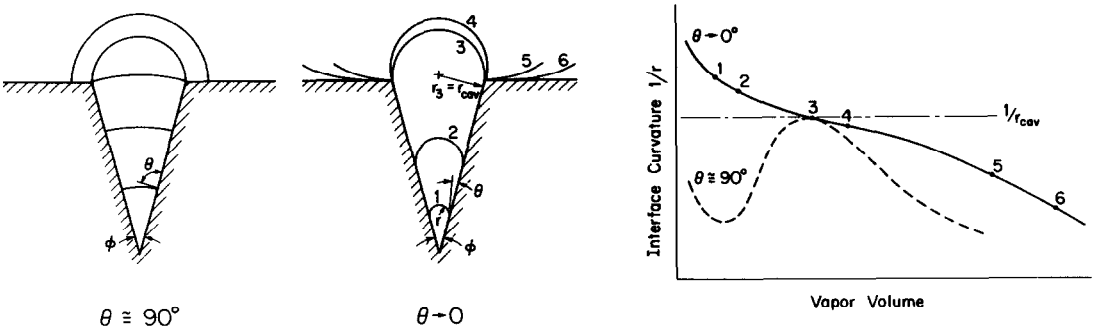


FIG. 13. Schematic representation of vapor embryo growth for highly wetting and non-wetting fluids.

Low surface tension fluids tend to splash liquid off their wave crests, reducing the film flow rate and the convective heat transfer coefficient.

(2) Incipience in falling water films is strongly influenced by turbulent eddies and interfacial waves which together suppress nucleation from surface cavities, requiring higher wall superheat for incipience compared to other forced convection systems. A new semi-empirical model was developed to account for these important effects using physical parameters utilized in commonly accepted incipience models.

(3) The low contact angle of FC-72 allows the liquid film to flood wall cavities, resulting in very small vapor embryos in the heated wall. These embryos require much higher wall superheat than predicted from incipience theory. It was found that the incipient superheat in highly wetting fluids is more dependent on vapor embryo size than cavity radius. This dependence may be complicated by vapor entrainment from the film interface due to wave-induced churning prior to boiling.

*Acknowledgement*—The authors gratefully acknowledge the support of the Office of Basic Sciences of the U.S. Department of Energy (Grant No. DE-FG02-85ER13398).

## REFERENCES

1. W. Wilke, Warmeubergang an rieselfilme, *VDI ForschHft.* 490 (1962).
2. G. Gimbutis, Heat transfer of a turbulent falling film, *Proc. 5th Int. Heat Transfer Conf.*, Tokyo, Japan, Vol. 2, pp. 85–89 (1974).
3. G. J. Gimbutis, A. J. Drobacivius and S. S. Sinkunas, Heat transfer of a turbulent water film at different initial flow conditions and high temperature gradients, *Proc. 6th Int. Heat Transfer Conf.*, Toronto, Canada, Vol. I, pp. 321–326 (1978).
4. T. Fujita and T. Ueda, Heat transfer to falling liquid films and film breakdown—I, *Int. J. Heat Mass Transfer* **21,** 97–108 (1976).
5. P. H. Oosthuzien and T. Cheung, An experimental study of heat transfer to developing water film flow over cylinders, *J. Heat Transfer* **99,** 152–155 (1977).
6. J. A. Shmerler and I. A. Mudawwar, Local heat transfer coefficient in wavy free-falling turbulent liquid films undergoing uniform sensible heating, *Int. J. Heat Mass Transfer* **31,** 67–77 (1988).
7. K. R. Chun and R. A. Seban, Heat transfer to evaporating liquid films, *J. Heat Transfer* **93,** 391–396 (1971).
8. T. Fujita and T. Ueda, Heat transfer to falling liquid films and film breakdown—II, *Int. J. Heat Mass Transfer* **21,** 109–118 (1976).
9. J. A. Shmerler and I. A. Mudawwar, Local evaporative heat transfer coefficient in turbulent free-falling liquid films, *Int. J. Heat Mass Transfer* **31,** 731–742 (1988).
10. R. Mesler, Nucleate boiling in thin liquid films. In *Boiling Phenomena* (Edited by S. Van Stralen and R. Cole), Vol. 2, pp. 813–819. Hemisphere, Washington, DC (1976).
11. M. Cerza and V. Sernas, Nucleate boiling heat transfer in developing laminar falling water films, *Proc. ASME–JSME Thermal Engng Joint Conf.*, Honolulu, Hawaii, Vol. I, pp. 111–118 (1983).
12. M. Cerza and V. Sernas, Boiling nucleation criteria for a falling water film. In *Multiphase Flow and Heat Transfer*, HTD-Vol. 47, pp. 111–116. ASME (1985).
13. T. Sato and H. Matsumura, On the conditions of incipient subcooled boiling and forced-convection, *Bull. J.S.M.E.* **7,** 392–398 (1963).
14. A. E. Bergles and W. M. Rohsenow, The determination of forced convection surface-boiling heat transfer, *J. Heat Transfer* **86,** 365–372 (1964).
15. E. J. Davis and G. H. Anderson, The incipience of nucleate boiling in forced convection flow, *A.I.Ch.E. Jl* **12,** 774–780 (1966).
16. S. T. Yin and A. H. Abdelmessih, Prediction of incipient flow boiling from a uniformly heated surface, *A.I.Ch.E. Symp. Ser.* **164,** 236–243 (1974).
17. R. Hino and T. Ueda, Studies on heat transfer and flow characteristics in subcooled flow boiling—Part I. Boiling characteristics, *Int. J. Multiphase Flow* **11,** 269–281 (1985).
18. Y. Sudo, K. Miyata, H. Ikawa and M. Kaminaga, Experimental study of incipient nucleate boiling in narrow vertical rectangular channel simulating subchannel of upgraded JRR-3, *J. Nucl. Sci. Technol.* **23,** 73–82 (1986).
19. C. V. Han and P. Griffith, The mechanism of heat transfer in nucleate pool boiling—I, *Int. J. Heat Mass Transfer* **8,** 887–904 (1965).
20. W. Frost and G. S. Dzakowic, An extension of the method of predicting incipient boiling on commercially finished surfaces, ASME Paper No. 67-HT-61 (1967).
21. A. E. Bergles and M. C. Chyu, Characteristics of nucleate pool boiling from porous metallic coatings, *J. Heat Transfer* **104,** 279–285 (1982).
22. P. J. Marto and V. J. Lepere, Pool boiling heat transfer from enhanced surfaces to dielectric fluids, *J. Heat Transfer* **104,** 292–299 (1982).
23. K. P. Moran, S. Oktay, L. Buller and G. Kerjilian, Cooling concept for IBM electronic packages, *IEPS Proc.* 120–140 (1982).
24. A. S. Hodgson, Hysteresis effects in surface boiling of water, *J. Heat Transfer* **91,** 160–162 (1969).
25. A. Bar-Cohen and T. W. Simon, Wall superheat excur-

sion in the boiling incipience of dielectric fluids. In *Heat Transfer in Electronic Equipment*, HTD-Vol. 57, pp. 83–94. ASME (1986).
26. T. M. Anderson and I. A. Mudawwar, Microelectronic cooling by enhanced pool boiling of a dielectric fluorocarbon liquid, *ASME Proc. 1988 Natl Heat Transfer Conf.*, HTD—Vol. 96, pp. 551–560, Houston, Texas (1988).
27. D. E. Maddox and I. A. Mudawwar, Single and two-phase convective heat transfer from smooth and enhanced microelectronic heat sources in a rectangular channel, *ASME Proc. 1988 Natl Heat Transfer Conf.*, HTD—Vol. 96, pp. 533–542, Houston, Texas (1988).
28. J. J. Lorenz, B. B. Mikic and W. M. Rohsenow, Effects of surface condition on boiling characteristics, *Proc. 5th Int. Heat Transfer Conf.*, Tokyo, Japan, Vol. 4, pp. 35–39 (1974).
29. I. A. Mudawwar, T. A. Incropera and F. P. Incropera, Microelectronic cooling by fluorocarbon liquid films, *Proc. Int. Symp. on Cooling Technology for Electronic Equipment*, Honolulu, Hawaii, pp. 340–357 (1987).
30. S. Toda and H. Uchida, Study of liquid film cooling with evaporation and boiling, *Trans. J.S.M.E.* **38**, 1830–1838 (1972).

## PREDICTION DE L'APPARITION DE L'EBULLITION NUCLEEE DANS DES FILMS TOMBANTS, LIQUIDES, TURBULENTS AVEC ONDULATIONS

**Résumé**—Des expériences sont faites pour développer la compréhension de l'ébullition naissante dans des films tombants, liquides, turbulents avec ondulations. Les conditions d'apparition dans des films sont mesurées et mises en formules pour l'eau et le fluorocarbure (FC-72). L'apparition dans des films d'eau est influencée par des tourbillons turbulents et, de façon plus générale, par des vagues en surface. On présente une nouvelle approche pour prédire la naissance dans l'eau et autres fluides non mouillants. Cette approche utilise des paramètres physiques de modèles communément acceptés et elle fournit le moyen de corriger ces modèles pour les effets des tourbillons turbulents et les vagues en rouleau. Cette étude montre aussi quelques caractéristiques uniques d'apparition pour les films de FC-72. Les faibles forces de tension interfaciale du FC-72 conduisent à la rupture de la crête des vagues en rouleau avant et pendant l'ébullition nucléée. Le faible angle de contact de FC-72 conduit à une pénétration profonde dans les cavités de la paroi. La naissance à partir de ces cavités noyées nécessite une surchauffe de paroi plus élevée que ce qui est prédit par les modèles d'apparition.

## BERECHNUNG DES SIEDEBEGINNS IN WELLIGEN, FREI FALLENDEN TURBULENTEN FLÜSSIGKEITSFILMEN

**Zusammenfassung**—Um ein grundlegendes Verständnis für den Siedebeginn in welligen, frei fallenden turbulenten Flüssigkeitsfilmen zu entwickeln, wurden Versuche durchgeführt. Die Bedingungen beim Siedebeginn wurden für Wasser und einen Fluorkohlenstoff (FC-72) gemessen und korreliert. Der Siedebeginn wird in Wasserfilmen durch Turbulenzwirbel und stärker noch durch Oberflächenwellen beeinflußt. Es wird eine neue Möglichkeit aufgezeigt, den Siedebeginn in Wasser und anderen nicht benetzenden Flüssigkeiten zu berechnen. Bei dieser Methode werden physikalische Parameter von allgemein anerkannten Modellen zum Siedebeginn benutzt und mit Korrekturen für den Einfluß der Turbulenz und der Oberflächenwellen versehen. Diese Untersuchung zeigt auch einige eigenartige Eigenschaften bezüglich des Siedebeginns in Fluorkohlenstoff-Filmen. Die geringen Oberflächenspannungskräfte von FC-72 erlauben vor und während des Blasensiedens, daß Tropfen und Flüssigkeitssträhnen den Kamm einer ankommenden Welle aufbrechen. Der kleine Randwinkel von FC-72 gestattet der Flüssigkeit, weit in die Vertiefungen der Heizfläche vorzudringen. Aus diesem Grund sind bei derart gefluteten Vertiefungen beim Siedebeginn weitaus größere Übertemperaturen erforderlich als die mit Modellen berechneten.

## НАЧАЛЬНЫЙ ПЕРИОД ПУЗЫРЬКОВОГО КИПЕНИЯ В ВОЛНООБРАЗНЫХ СВОБОДНО СТЕКАЮЩИХ ТУРБУЛЕНТНЫХ ПЛЕНКАХ ЖИДКОСТИ

**Аннотация**—Проведено экспериментальное исследование для выяснения процесса зарождения кипения в волнообразных свободно стекающих турбулентных пленках жидкости. Выполнены измерения и сопоставлены условия начала кипения в воде и жидком фторуглероде (ФУ-72). На кипение водяной пленки влияние оказывают турбулентные вихри и, еще в большей степени, волны на межфазной границе. Предложен новый подход к расчету зарождения кипения в воде и других несмачивающих стенку жидкостях, основанный на физических параметрах известных моделей зарождения кипения и позволивший внести в них поправку на эффекты турбулентных вихрей и валов. Также отмечены некоторые специфические характеристики исследуемого процесса в пленках фторуглерода. Так как силы поверхностного натяжения ФУ-72 малы, капли и жидкие струйки срываются с гребней набегающих валов до и в процессе пузырьового кипения. Из-за небольшого угла смачивания ФУ-72 жидкость глубоко проникает в микропоры стенки. Таким образом, для образования пузырьков в этих микропорах требуется перегрев стенок, значительно превышающий рассчитываемый по общепринятым моделям.